LAF | https://doi.org/10.15302/J-LAF-2026-0004
Volume 14 / Issue 1 / 260004 / 2026
Received Date | 2025-04-05 Accepted Date | 2025-08-29

Responses of Urban Flood Resilience to Climate Change and Its Multi-Level Enhancement Pathway

Jiaxuan ZHENG[1,2,*], Zhijun YAO[3], Xianghua LIAO[4], Guoru HUANG[4,5,6], Xi CHEN[7]

1 Department of Hydraulic Engineering, School of Civil Engineering, Tsinghua University, Beijing 100084, China
2 State Key Laboratory of Hydroscience and Engineering, Tsinghua University, Beijing 100084, China
3 Guangdong Provincial Academy of Building Research Group Co., Ltd., Guangzhou 510500, China
4 School of Civil Engineering and Transportation, South China University of Technology, Guangzhou 510640, China
5 State Key Laboratory of Subtropical Building and Urban Science, South China University of Technology, Guangzhou 510640, China
6 Guangdong Engineering Technology Research Center of Safety and Greenization for Water Conservancy Project, Guangzhou 510640, China
7 Department of Civil and Earth Resources Engineering, Graduate School of Engineering, Kyoto University, Kyoto 612-8235, Japan

*CORRESPONDING AUTHOR
Address: New Hydraulic Engineering Building, No. 30 Shuangqing Road, Haidian District, Beijing 100084, China
Email: zhengjx@mail.tsinghua.edu.cn

GRAPHICAL ABSTRACT

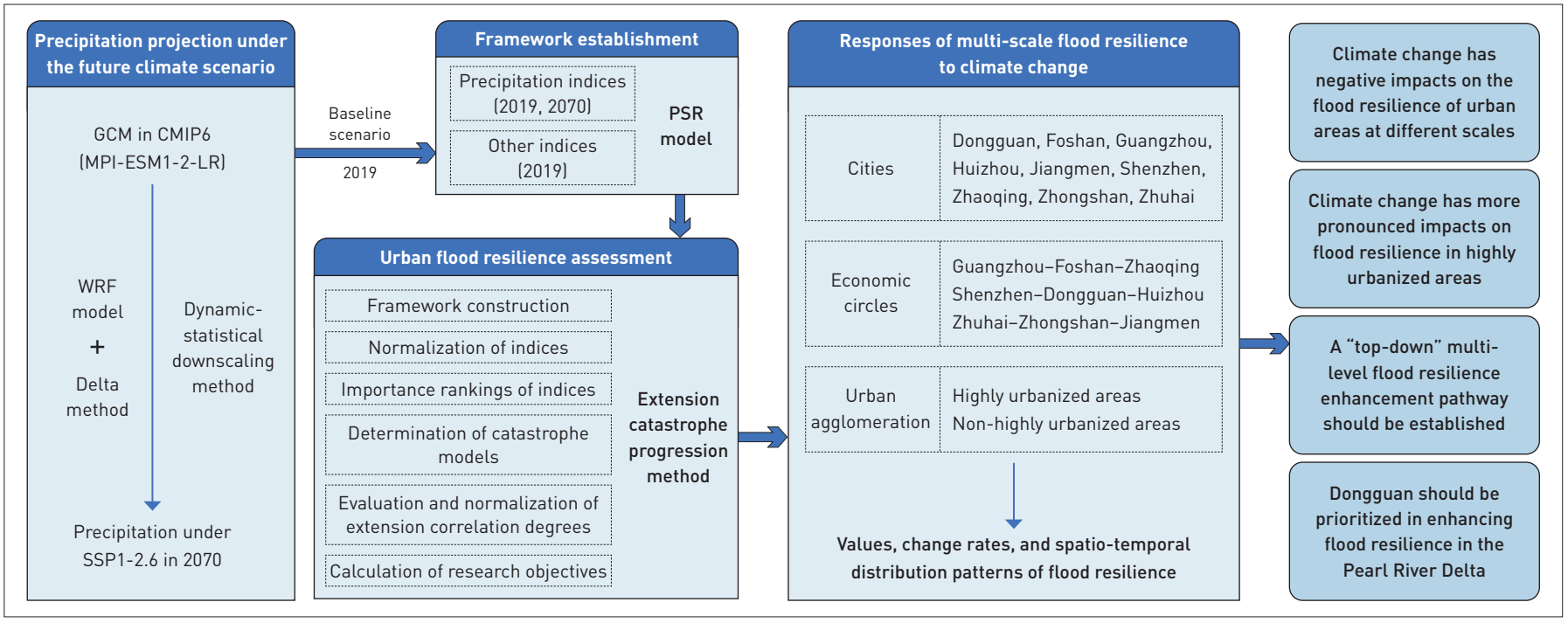

ABSTRACT

Driven by climate change, extreme events such as floods are becoming increasingly frequent globally. To address the growing and dynamic flood risks and foster the development of resilient cities, the concept of urban flood resilience has been increasingly applied to flood prevention. Investigating multi-scale responses of urban flood resilience to climate change can help policymakers develop multi-level enhancement pathways and concrete measures to enhance flood resilience, providing guidance for urban flood risk management. However, research in this field remains insufficient. Therefore, taking the Pearl River Delta (PRD) as the target area,

this study applied the pressure–state–response (PSR) model and the extension catastrophe progression method to assess urban flood resilience in 2019 and 2070 under SSP1-2.6. From the perspectives of the city, economic circle, and urban agglomeration, the impacts of climate change on multi-scale urban flood resilience and multi-level enhancement pathways for flood resilience of the PRD were investigated. Results show that its response of flood resilience to climate change is most evident in Zhuhai and least evident in Shenzhen. Climate change exerts its strongest impacts on the flood resilience of the Shenzhen–Dongguan–Huizhou (SDH) economic circle and the weakest on the Guangzhou–Foshan–Zhaoqing economic circle. Across all scales, climate change impedes the maintenance of flood resilience in the PRD, even under a low-emission sustainable development scenario. This impact is more pronounced in highly urbanized areas than in less urbanized ones. Consequently, the PRD should establish a "top-down" multi-level approach of "highly urbanized areas–the SDH economic circle–Dongguan" for flood resilience enhancement. Strengthening the flood resilience of Dongguan is of significant importance for achieving the overall enhancement in the PRD under climate change.

KEYWORDS

Urban Flood Resilience; Climate Change; Multi-level; Pressure-State-Response Model; Pearl River Delta

HIGHLIGHTS

- Analyzes flood resilience responses to climate change at the scales of city, economic circle, and urban agglomeration
- Proposes multi-level enhancement pathways for flood resilience in the Pearl River Delta
- Climate change has negative impacts on the flood resilience of urban areas at different scales
- Enhancing flood resilience in the Pearl River Delta should focus on Dongguan

RESEARCH FUNDS

- National Natural Science Foundation of China (No. 52279015)
- State Key Laboratory of Subtropical Building and Urban Science (No. 2023ZA01)

1 Introduction

In recent years, the intensification of climate change has been accompanied by a rising frequency of short-duration extreme rainfall and prolonged heavy precipitation events at the global scale. Coupled with urban expansion, which has transformed extensive permeable surfaces into impervious ones, the natural urban hydrological cycle has undergone profound alterations, thereby amplifying the incidence of extreme hazards such as urban flooding[1]. The rapid developments of society and economy have led to a high concentration of population and assets, making disaster-prone areas increasingly vulnerable. To address the growing severity of flooding under climate change, and in line with the current global trend toward resilient cities, the concept of urban flood resilience emerged as a key focus, particularly in relation to large urban agglomerations such as the Pearl River Delta (PRD)[2].

Climate change and urban flood resilience have become major research focuses, generating a substantial body of scholarship worldwide. Current climate change research relies on global climate models (GCMs) to project future changes in meteorological variables (e.g., precipitation, temperature). To improve the reliability of GCMs, support their development, and advance the understanding of the Earth's climate system[3], the World Climate Research Programme launched the Coupled Model Intercomparison Project (CMIP), which has now completed its sixth phase (CMIP6). Compared with earlier phases, CMIP6 proposed new future climate projection scenarios and incorporated them in a sub-project—the Scenario Model Intercomparison Project (Scenario MIP)[4]. Scenario MIP adopted a matrix framework that combined the shared socioeconomic pathways with representative concentration pathways (SSP–RCPs), placing a greater emphasis on consistency between future radiative forcing and shared socioeconomic scenarios. The core future scenarios included in Scenario MIP are SSP1-2.6, SSP2-4.5, SSP3-7.0, and SSP5-8.5. Given the generally coarse spatial resolution of GCMs, scholars worldwide have utilized the dynamic downscaling[5], statistical downscaling[6], and dynamic-statistical downscaling methods[7] to enhance the projection accuracy of GCMs of meteorological factors, providing a basis for flood risk prediction[8] and flood resilience response[9]. Moreover, relevant research indicated that the combined dynamic–statistical downscaling method leverages the strengths of both methods[10]. By maintaining a sound physical and dynamical foundation while referring to extensive historical climate data, this method enables higher-precision downscaling of climate factors and facilitates the assessment of future flood risk.

Regarding urban flood resilience, current quantitative analyses primarily rely on its inherent nature, including the resistance, adaptation, and recovery capabilities demonstrated by urban systems during flooding[11]. These analyses have gradually established evaluation approaches centered on index-based and system performance curve-based methods[12–13], as well as various frameworks such as the pressure–state–response (PSR) model. The index-based method serves as the primary tool for assessing flood resilience at larger spatial scales (e.g., cities, urban agglomerations). For instance, Wenjie Chen et al. established a PSR model-based urban flood resilience assessment framework in the PRD to compare and analyze flood resilience in 1990 and 2020 in terms of the evolution of spatio-temporal patterns[14]. Gang Liu et al. conceptualized urban flood resilience as the joint outcome of the stimulatory nature of the pressure layer, the sensitivity of the state layer, and the adaptability of the response layer, and selected resilience indices accordingly[15]. Juan Ji et al. constructed a PSR model-based urban flood resilience assessment framework for Jiangsu Province, and evaluated resilience and its influencing factors using the projection pursuit model and grey relational analysis method[16]. Despite these advancements, significant knowledge gaps remain in planning pathways of flood resilience enhancement. Because the impacts of climate change on flood disasters vary across spatial scales[17], urban flood resilience responses are inherently scale-dependent. Exploring these multi-scale responses is essential for developing multi-level flood resilience enhancement planning pathways, such as the "top-down" approach that can be optimized step-by-step across varying administrative and geographical levels. However, research in this area remains limited. Therefore, it is urgent to conduct more extensive and in-depth explorations into the multi-scale flood resilience responses of under climate change, as well as the pathways for enhancing resilience[18].

In 2020, the *CPC Central Committee's Proposal for Formulating the 14th Five-Year Plan for National Economic and Social Development and the Long-Range Objectives Through the Year 2035* were adopted and first proposed the concept of developing resilient cities in China. In response to future climate change, the Chinese government has placed a high priority on enhancing urban resilience. However, most Chinese cities currently show low resilience[19–20], which poses a critical challenge to urban disaster prevention and mitigation. To bridge this gap, it is important to clarify the impact of climate change on urban flood resilience and propose scientific flood resilience enhancement pathways. Such measurements are essential to strengthen the capacity of cities to resist, adapt to, and recover from climate-induced stresses, facilitating sustainable urban development. Therefore, this study aims to address the current research gaps in flood resilience responses of urban areas at multiple scales in the context of climate change, as well as the multi-scale pathways for enhancing flood resilience. Related research indicate that the increase in average annual precipitation in the PRD under SSP1-2.6 is smaller than that under other climate change scenarios in the near future[10]. Accordingly, the evolution of flood resilience in the PRD under SSP1-2.6 relative to the baseline exhibits distinctive characteristics. It serves as a benchmark for understanding the fundamental trajectory of flood resilience under the most favorable development pathway and provides essential guidance for enhancing flood resilience in the PRD under climate change. On this basis, this study first applied the dynamic-statistical downscaling method to project the precipitation distribution under the SSP1-2.6 scenario for the key year 2070 in the near future. The PSR model and extension catastrophe progression method (ECPM) were subsequently employed to assess and compare the flood resilience at three scales—city, economic circle, and urban agglomeration—under the baseline (2019) and future scenarios. The responses of flood resilience to climate change at different scales were thereby investigated, and the multi-level enhancement pathways for flood resilience were proposed. The findings offer guidance for improving urban flood resilience, supporting disaster risk reduction, and promoting the development of resilient cities under the threat of climate change.

2 Study Area and Methods

2.1 Study Area

The PRD is located in the south-central part of Guangdong Province, China and comprises nine cities: Dongguan, Foshan, Guangzhou, Huizhou, Jiangmen, Shenzhen, Zhaoqing, Zhongshan, and Zhuhai. It is one of the three largest urban agglomerations in China, and has formed three major economic circles: the Guangzhou–Foshan–Zhaoqing (GFZ) economic circle with Guangzhou as the core, the Shenzhen–Dongguan–Huizhou (SDH) economic circle with Shenzhen as the core, and the Zhuhai–Zhongshan–Jiangmen (ZZJ) economic circle with Zhuhai as the core. According to the *Guangdong Statistical Yearbook* (2024), the PRD encompasses a total area of 54,767 km^2 as of 2023. The World Bank Group reported that the PRD had emerged as the world's largest metropolitan area by population and land area in 2015[21]. As one of the most developed regions in China, the PRD has undergone significant land use changes over time, with urbanization driving

substantial expansion of built-up areas[22]. This process has resulted in the formation of highly urbanized areas[23], mainly located in Dongguan, Foshan, Guangzhou, Shenzhen, Zhongshan, and Zhuhai. These areas serve as the primary population concentration and inflow zones of the PRD and play a key role in its economic and social development.

2.2 Methods

First, combining CMIP6 GCM data with the mesoscale Weather Research and Forecasting (WRF) model[24], this study employed dynamic–statistical downscaling method to project future precipitation in the PRD. Next, a PSR model-based urban flood resilience evaluation system incorporating precipitation indices was established, and the ECPM was adopted to assess the region's urban flood resilience under different scenarios.

2.2.1 Dynamic–Statistical Downscaling Method

Given its proved superior performance and suitability for the PRD[10], the dynamical–statistical downscaling method was employed to estimate future climate conditions in this study. The research first applied the WRF model to dynamically downscale GCM daily data. The WRF model has been extensively applied in the PRD for precipitation projection and studies on urban flooding[8,25], featuring high flexibility and a modular architecture[26]. Compared with global models like the US Global Forecast System (GFS), WRF offers multi-level nesting for fine-scale meteorological forecasts and benefits from open-source code for secondary development, but it requires complex parameter configurations and a time-consuming tuning process. The resulting outputs were then statistically downscaled using the Delta method[27] to derive the spatial distribution of daily precipitation over the study area in the future period. The detailed calculation procedure is given in Eq. (1):

$$P_R''(d) = P_R(d) \times (P_d''(m) / P_d(m)), \quad (1)$$

where $P_R''(d)$ is the future daily precipitation (mm) in the study area derived from GCM dynamical–statistical downscaling; $P_R(d)$ is the observed daily precipitation (mm) in the study area in the reference period; $P_d''(m)$ and $P_d(m)$ represent the monthly precipitation (mm) in the study area derived from GCM dynamic downscaling in the future and reference periods, respectively.

2.2.2 PSR Model

The PSR model was proposed by David J. Rapport and Tony Friend, and was subsequently further developed and refined jointly by the Organisation for Economic Co-operation and Development (OECD) and the United Nations Environment Programme (UNEP)[28]. It reflects the interactions between humans and the environment and addresses three fundamental questions of sustainability: what has happened, why it has happened, and how it should be addressed[28]. The indices in the model should be selected based on three criteria—pressure, state, and response—aligned with the research objectives. The model has recently been widely applied in environmental studies such as urban flood risk and resilience evaluation[14–15,29–30].

2.2.3 Extension Catastrophe Progression Method

The traditional catastrophe progression method, based on catastrophe theory and fuzzy mathematics, is frequently applied to comprehensive assessment, ranking, and analysis of research objectives. Although it does not require subjective weight assignment for index ranking, the relative importance of indices at the same level depends on expert experience, thereby imparting subjectivity to the outcomes. Na Li et al. introduced the extenics theory to improve the traditional catastrophe progression method and proposed the extension catastrophe progression method[31]. Referring to previous research[28,32], this method utilizes entropy values to objectively rank indices, mitigating subjectivity and uncertainty of the outcomes, while overcoming the restriction of the traditional method that limits the number of control variables to four. Its application in this study involves seven steps: 1) construction of the PSR model-based assessment framework; 2) indices normalization using the extremum method; 3) importance rankings of indices using the entropy method; 4) determination of catastrophe models; 5) evaluation of extension correlation degrees based on the extremum method; 6) normalization of extension correlation degrees; and 7) calculation of the research objective.

2.2.3.1 Construction of the Assessment Framework

After defining the research objective, representative, scientific, accessible, and relatively simple-to-calculate indices were selected to construct the evaluation framework. The framework was designed to exhibit a clear hierarchical structure and to reflect the dynamics and integrity of the evaluation system.

2.2.3.2 Indices Normalization

This step first distinguished the attributes of the selected indices, i.e., determining whether each index is positive or negative in relation to the research objective. The extremum method was subsequently applied to standardize the indices. The normalization procedure for indices with different attributes were defined as Eq. (2):

$$x_{ij}^{'}=\begin{cases}\dfrac{x_{ij}-x_{\min}^{j}}{x_{\max}^{j}-x_{\min}^{j}}\alpha+\beta, \text{positive index}\\ \dfrac{x_{\max}^{j}-x_{ij}}{x_{\max}^{j}-x_{\min}^{j}}\alpha+\beta, \text{negative index}\end{cases}, \quad (2)$$

where x_{ij} is the initial value of the j-th sample in the i-th index; x_{ij}' is the normalized value of x_{ij}; α and β are parameters that determine the upper and lower limits of x_{ij}', respectively.

2.2.3.3 Importance Rankings of Indices

Based on the normalized index values, this step applied the entropy method to determine the importance ranking of indices, with their entropy values calculated using Eq. (3):

$$e_i=-K_i\sum_{j=1}^{m_i}y_{ij}\ln y_{ij}, \quad (3)$$

where e_i is the entropy value of the i-th index; m_i is the total number of samples for the i-th index; K_i is a normalization coefficient ensuring that the calculation value ranges between 0 and 1 for the i-th index; and y_{ij} is the proportion of the normalized value of x_{ij} to the sum of all normalized values for the i-th index. According to the principle of information entropy, indices with lower entropy values were considered to be more important. K_i and y_{ij} were calculated as follows:

$$K_i=\frac{1}{\ln m_i}, \quad (4)$$

$$y_{ij}=\frac{x_{ij}^{'}}{\sum_{i=1}^{m}x_{ij}^{'}}. \quad (5)$$

Equations (3, 5) imply that x_{ij} and y_{ij} should be greater than 0. Therefore, α and β in Eq. (2) were set to 0.9 and 0.05, respectively[32].

2.2.3.4 Determination of Catastrophe Models

In the ECPM, objects at each level are abstracted as state or control variables, with each state variable encompassing multiple control variables. Indices serve as control variables, with their criteria acting as the state variables, while criteria function as control variables with the research objective as the state variable. Catastrophe models are classified according to the number of control variables under a given state variable, with the cusp, swallowtail, and butterfly models corresponding to two, three, and four control variables, respectively. To meet this requirement, the number of control variables should be limited to two to four; if it exceeds four, variables are subdivided based on their relative importance to determine the appropriate catastrophe model type.

2.2.3.5 Evaluation of Extension Correlation Degrees

The extension correlation degree of each index should be positively correlated with the research objective, with values ranging from 0 to 1. If the index i is a positive index in the range of a to b, the extension correlation degree k of its sample j should be calculated using Eq. (6). If the index i is a negative index, the extension correlation degree k of its sample j should be calculated using Eq. (7):

$$k(x_{ij})=\frac{x_{ij}-a}{b-a}, \quad (6)$$

$$k(x_{ij})=\frac{b-x_{ij}}{b-a}. \quad (7)$$

2.2.3.6 Normalization of Extension Correlation Degrees

The normalization approach for the extension correlation degree of each index is determined by the type of corresponding catastrophe model and the relative importance of the index within the layer, as detailed in Table 1. In the equations, x denotes the state variable, while u, v, w, and t represent the control variables, and x_u, x_v, x_w, and x_t are the normalized extension correlation degree of u, v, w, and t. The significance of u, v, w, and t decreases sequentially.

2.2.3.7 Calculation of Research Objectives

The calculation of the research objective is based on the normalized extension correlation degrees of the indices. According to the catastrophe model type and the relationships among control variables, the corresponding state variable is calculated using either the minimum or the average of its control variables (Table 2), with variable definitions and values given in Table 1. Following the calculation methods in Table 2, each criterion is first derived from the normalized extension correlation degrees of its indices, which

Table 1: Basic information of the catastrophe models

Catastrophe model	Potential function	Normalization function
Cusp	$y=x^4+ux^2+vx$	$x_u=\sqrt{k(u)}, x_v=\sqrt[3]{k(v)}$
Swallowtail	$y=x^5+ux^3+vx^2+wx$	$x_u=\sqrt{k(u)}, x_v=\sqrt[3]{k(v)}, x_w=\sqrt[4]{k(w)}$
Butterfly	$y=x^6+ux^4+vx^3+wx^2+tx$	$x_u=\sqrt{k(u)}, x_v=\sqrt[3]{k(v)}, x_w=\sqrt[4]{k(w)}, x_t=\sqrt[5]{k(t)}$

Table 2: Calculation methods of state variables in the catastrophe models

Catastrophe model	Relationship between control variables	
	Non-complementary	Complementary
Cusp	$\min(x_u, x_v)$	$(x_u + x_v)/2$
Swallowtail	$\min(x_u, x_v, x_w)$	$(x_u + x_v + x_w)/3$
Butterfly	$\min(x_u, x_v, x_w, x_t)$	$(x_u + x_v + x_w + x_t)/4$

Table 3: Scheme settings in the WRF model

Scheme category	Scheme setting	Source
Cumulus parameterization	Kain–Fritsh scheme	Ref. [35]
Long wave radiation	Rapid radiative transfer model (RRTM) scheme	Ref. [36]
Short wave radiation	Dudhia scheme	Ref. [37]
Boundary layer	Yonsei University (YSU) scheme	Ref. [38]
Microphysics	Lin et al. scheme	Ref. [39]
Land surface	Noah land surface model (Noah LSM)	Ref. [40]

are complementary within the same criterion level; the research objective is then determined by the values of its criteria, with criteria across levels also being complementary.

3 Case Study

3.1 Precipitation Projection in the PRD Under Future Climate Scenario

The precipitation projection for the PRD under future climate scenario was conducted using the dynamic–statistical downscaling method. Previous research has identified 2070 as a key milestone in the near future and an important year for assessing the long-term effects of climate change[8,10,33–34]. Accordingly, the future period in this paper was set as 2070. The initial and boundary conditions for the WRF model in this study were derived from MPI-ESM1-2-LR, one of the commonly used GCMs in CMIP6. The WRF model employed a single-layer grid configuration with a horizontal resolution of 20 km, divided into 45 vertical layers, and an atmospheric top pressure of 50 hPa[8]. The parameterization schemes used in the model are detailed in Table 3[35–40]. Previous research show that the WRF model with the above settings exhibits high accuracy in simulating historical rainfall, with results during 1980–2010 (reference period) closely matching meteorological station observations[10], making it suitable for subsequent analyses. The future climate scenario selected for this study is SSP1-2.6, which combines the Shared Socioeconomic Pathway (SSP1) and the Representative Concentration Pathway (RCP2.6), comprehensively considering the impacts of low vulnerability, low mitigation challenges, and low radiative forcing[4]. SSP1 represents a sustainable development pathway, where population structure evolves rapidly while the population growth rate remains low; RCP2.6 represents a low forcing pathway, indicating that radiative forcing stabilizes at approximately 2.6 W/m^2 by 2100.

3.2 Construction of a PSR Model-based Urban Flood Resilience Assessment Framework

3.2.1 Index Selection and Calculation

Urban flood resilience was regarded as the research objective in the PSR model and was characterized by multiple indices after consulting relevant literature[5,14,41–43] and considering the representativeness, availability, and computational feasibility of indices. The pressure layer included maximum daily precipitation (Rx1day), number of days with daily precipitation no less than 25 mm (R25mm), typhoon frequency (TF), digital elevation model (DEM), and slope (SL), which reflect climate and topographic factors related to urban flooding. Land use (LU) and distance to rivers (DTR) were chosen for the state layer to characterize the current flood resistance capacity of the urban system. For the response layer, GDP density (GD), population density (PD), road density (RDD), railway density (RYD), and distance to hospitals (DTH) were selected to capture the capacity of the urban system to respond during flooding and to reconstruct in the post-disaster stage.① When

① The datasets utilized in this study were derived from multiple sources: observed historical rainfalls for 2019 were collected from 28 meteorological stations across the PRD; future projections were obtained from CMIP6 models (1.875° resolution); tropical cyclone data were sourced from the CMA Tropical Cyclone Data Center; DEM data (30 m resolution) were retrieved from the University of Bristol data repository and slope data were further derived from DEM. Land use data (30 m resolution) were acquired from Zenodo; river distribution networks were extracted from Bigemap; GDP density (1 km resolution) was sourced from the Resource and Environment Science Data Platform, Chinese Academy of Sciences; population density (100 m resolution) was sourced from WorldPop; road and railway data were obtained from OpenStreetMap; and geographic locations of hospitals were retrieved from the Baidu Map Server.

evaluating flood resilience for the seven LU types in the study area (i.e., impervious area, grassland, cropland, shrub, forest, water, and barren), forest is recognized for its strong self-regulation, water for its capacity to regulate and accommodate surface runoff, whereas barren land has limited functions due to its undeveloped state and shows comparatively small functional loss[28]. Accordingly, LU was assigned values ranging from 1 to 5 in the order of 1) impervious areas; 2) cropland; 3) grassland; 4) shrub; and 5) forest, water, and barren. A higher value indicates that, under the same level of flood disturbance, the LU is less affected in maintaining its normal functions and characteristics.

This study employed a baseline scenario of 2019 and a future scenario of SSP1-2.6 in 2070 to evaluate the impacts of climate change on urban flood resilience (Figs, 1, 2). The Rx1day

Fig. 1 Spatial patterns of Rx1day and R25mm under two scenarios.
Fig. 2 Spatial patterns of indices excluding Rx1day and R25mm under the scenario of 2019.

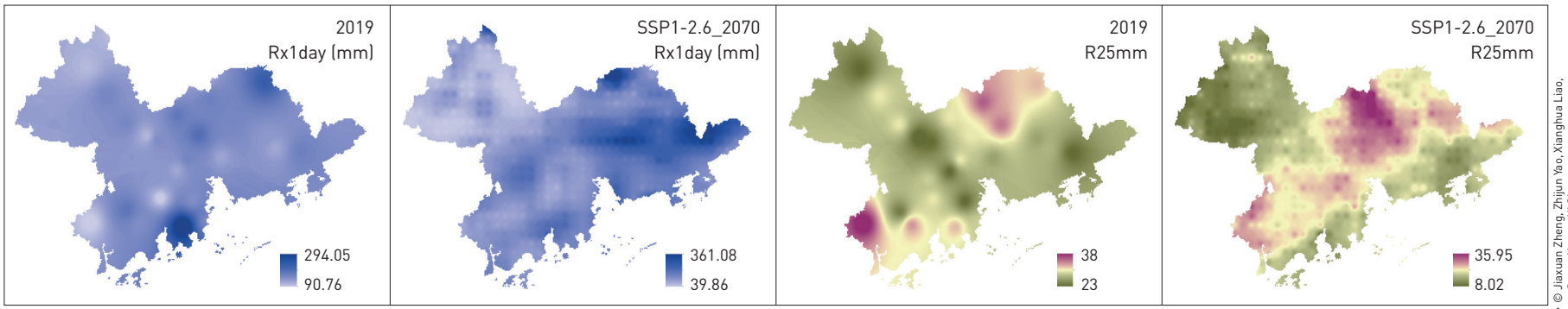

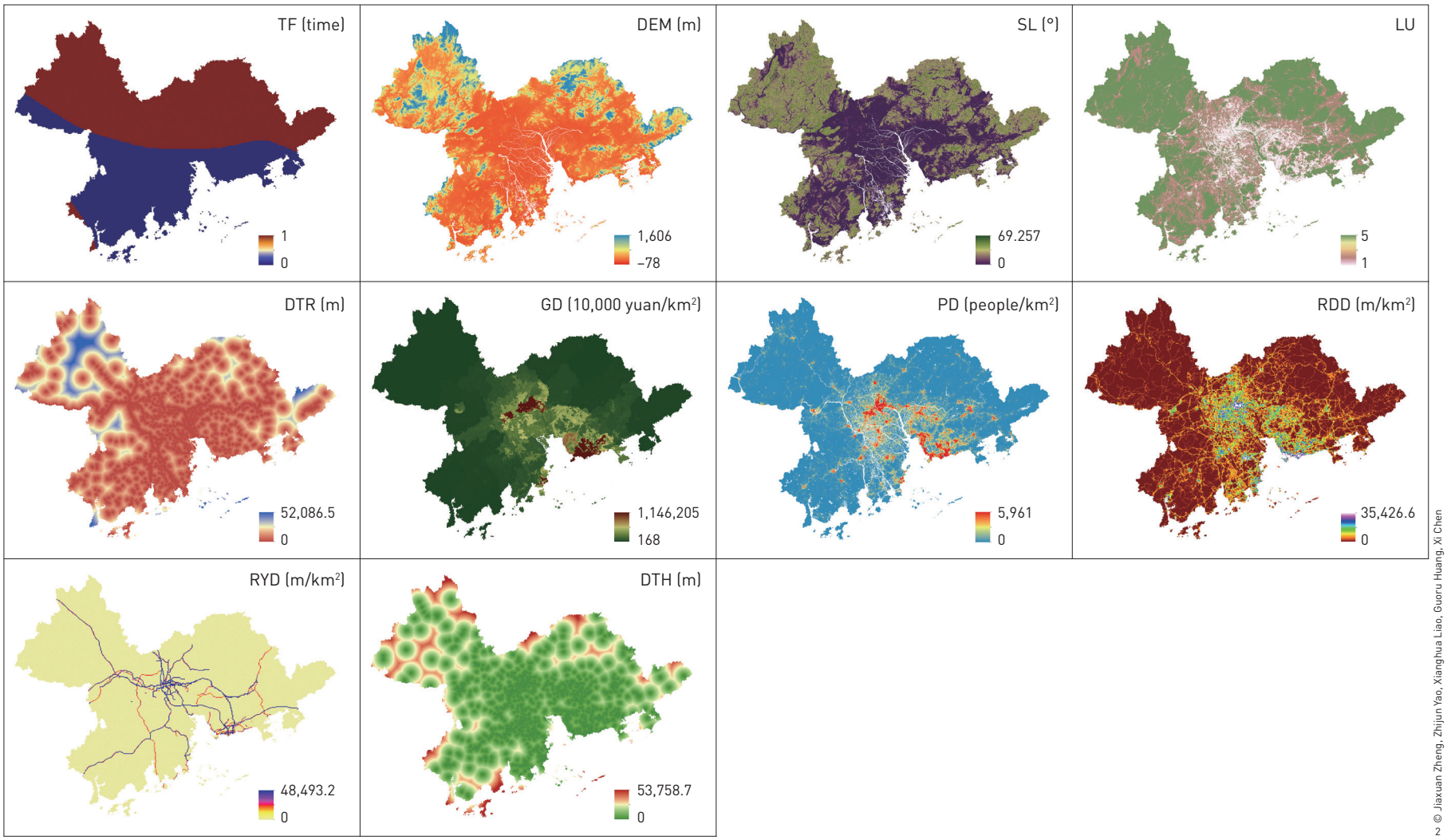

and R25mm in 2019 were calculated using observed data from meteorological stations in the study area, while those under the future scenario relied on the projected precipitation derived from the dynamic–statistical downscaling method (Fig. 1). Since this study primarily focuses on the impacts of precipitation changes caused by climate change on urban flood resilience, the spatial distributions of all indices except Rx1day and R25mm in the future scenario are consistent with those in the baseline (Fig. 2). As shown in Fig. 1, the high-value zones of Rx1day are mainly distributed in the southern and northeastern regions of the PRD in 2019, but shift to the central, eastern, and northern parts by 2070 under SSP1-2.6. The high-value areas of R25mm, concentrated in the southwest, south, and northeast in 2019, exhibit a northeast–southwest belt-shaped distribution in 2070. According to Fig. 2, high values of GD, PD, RDD, and RYD, as well as low values of LU are concentrated in the topographically flat central region of the PRD. These areas are also featured with relatively low surface elevation and proximity to rivers, with some parts have suffered typhoon damage in 2019.

3.2.2 Framework Establishment

Following the principles of the ECPM, indices in the pressure, state, and response layers were first ranked by importance based on their information entropy and the criteria layers were subsequently defined. The final urban flood resilience assessment framework under different scenarios and the catastrophe models for the various layers are illustrated in Fig. 3. The contribution attributes of the indices to flood resilience were determined based on the relevant literature[28]. It should be noted that for socio-economic indices (e.g., RDD, GD, RYD, PD), the assessment of urban flood resilience highlights their preventive and mitigating functions. Economic prosperity, population concentration, and transportation facilities constructed for human activities contribute not only to the response capacity during floods but also to post-disaster recovery and reconstruction. Accordingly, these four indices contribute positively to flood resilience in the assessment framework[14,28].

Fig. 3 Urban flood resilience assessment framework under two scenarios ("+" represents positive index, "–" represents negative index).

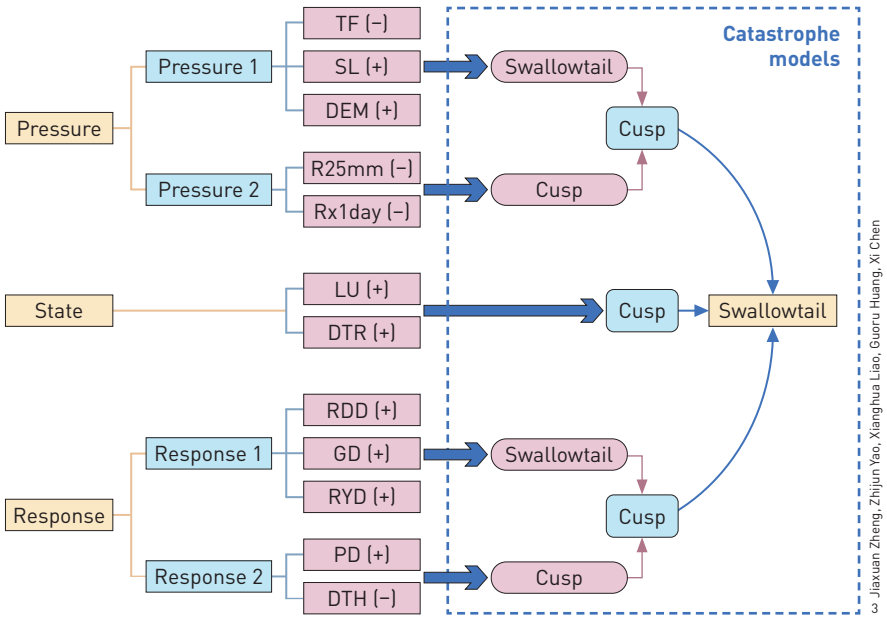

4 Multi-level Flood Resilience Enhancement Pathways Based on Multi-scale Responses to Climate Change

4.1 Multi-scale Flood Resilience Responses to Climate Change

4.1.1 City Scale

Taking the nine cities within the study area as statistical units, flood resilience was calculated at the city scale. Table 4 summarizes the flood resilience of each city under two scenarios, together with their respective rates of change. The ranking of cities by flood resilience, from highest to lowest, is Zhaoqing, Shenzhen, Jiangmen, Huizhou, Zhuhai, Zhongshan, Guangzhou, Foshan, and Dongguan in both the 2019 and the 2070 SSP1-2.6 scenario. In 2070, the projected flood resilience of all cities except Zhaoqing, Jiangmen,

Table 4: Flood resilience and its change rate of the cities under two scenarios

City	Area (km^2)	Flood resilience		Change rate (%)
		2019	SSP1-2.6 in 2070	
Dongguan	2,460.38	0.6104	0.6058	–0.76
Foshan	3,797.79	0.6227	0.6184	–0.69
Guangzhou	7,238.46	0.6367	0.6336	–0.49
Huizhou	11,350.36	0.6703	0.6678	–0.38
Jiangmen	9,535.19	0.6709	0.6724	0.22
Shenzhen	1,987.00	0.6740	0.6732	–0.12
Zhaoqing	14,891.43	0.6957	0.6979	0.32
Zhongshan	1,780.99	0.6414	0.6388	–0.42
Zhuhai	1,725.02	0.6567	0.6672	1.60

and Zhuhai shows a decreasing trend. This is primarily because the adverse effects of future precipitation changes on these three cities are weaker than other cities. Specifically, following the calculation principles of the ECPM, the values of Rx1day and R25mm in the pressure layer exhibit an increase under SSP1-2.6 when calculating flood resilience. As indicated by the absolute values of change rates, the response of flood resilience to climate change is most pronounced in Zhuhai but least pronounced in Shenzhen. The ranking of the remaining cities, from highest to lowest, is Dongguan, Foshan, Guangzhou, Zhongshan, Huizhou, Zhaoqing, and Jiangmen. Overall, climate change hinders the ability of most cities in the PRD to maintain their resilience to flooding, even under a low-emission scenario on a sustainable development path.

4.1.2 Economic Circle Scale

Taking the three economic circles as the statistical units, flood resilience was calculated. According to Table 5, the ranking of economic circles by flood resilience, from highest to lowest, is the GFZ, the ZZJ, and the SDH economic circles in both the 2019 and the 2070 SSP1-2.6 scenario. Despite the slight change, the flood resilience of the GFZ and the SDH economic circles in the SSP1-2.6 scenario in 2070 is lower than that in 2019. This suggests that the adverse effects of climate change on the capacity of the ZZJ economic circle to tolerate, adapt to, and recover from flooding are less pronounced than in other economic circles. This is because, under SSP1-2.6, flood resilience of Zhuhai and Jiangmen increases, and their combined gains exceed the loss projected in Zhongshan in 2070. Guangzhou, Foshan, Dongguan, Zhuhai, and Zhongshan exhibit lower flood resilience compared with their corresponding economic circles in 2019. However, this pattern persists for all of these cities except Zhuhai in 2070, whose flood resilience slightly exceeds that of the ZZJ

Table 5: Flood resilience and its change rate in economic circles under two scenarios

Economic circle	Area (km^2)	Flood resilience		Change rate (%)
		2019	SSP1-2.6 in 2070	
The GFZ economic circle	25,927.68	0.6686	0.6684	−0.03
The SDH economic circle	15,797.74	0.6612	0.6585	−0.41
The ZZJ economic circle	13,041.20	0.6654	0.6671	0.26

economic circle. In terms of the magnitude of change, climate change exerts the strongest impacts on flood resilience of the SDH economic circle, followed by the ZZJ economic circle , while its impacts on the GFZ economic circle are the weakest. Climate change exerts positive effects on flood resilience in the ZZJ economic circle but negative effects in the GFZ and SDH regions.

Overall, climate change undermines the capacity of the two largest economic circles in the PRD (Table 5) to maintain flood resilience, even under a low-emission scenario on a sustainable development path.

4.1.3 Urban Agglomeration Scale

The spatial distributions of overall flood resilience of the PRD under two scenarios, assessed from the perspectives of urban agglomeration scale, are presented in Fig. 4. Compared with the baseline scenario, the overall distribution of flood resilience in the study area exhibits only slight changes under SSP1-2.6. Nevertheless, reductions in the maximum and minimum values

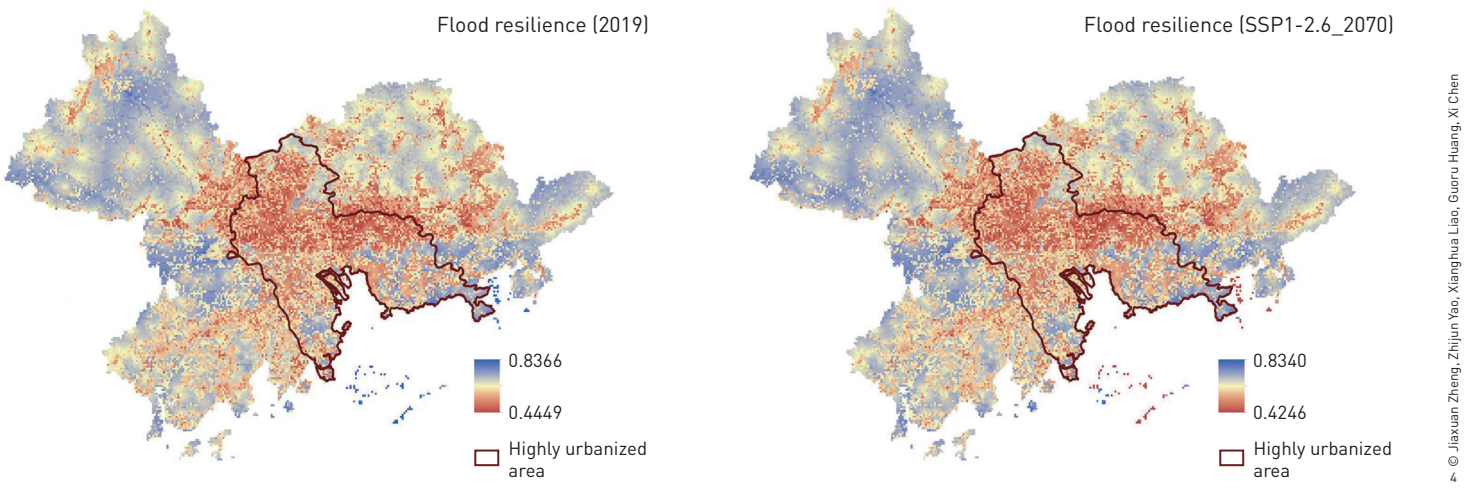

Fig. 4 Spatial patterns of flood resilience in the overall study area under two scenarios.

indicate that climate change weakens the capacity of the area to tolerate, adapt to, and recover from flooding. The low-value zones of flood resilience under both scenarios are concentrated in highly urbanized areas. Although developed economies and well-developed infrastructure in these areas facilitate the timely implementation of disaster prevention and mitigation measures and promote post-disaster recovery, their flat terrain, widespread impervious areas, and proximity to rivers make it more difficult to maintain pre-disaster operational conditions in flooding events than in other regions. Specifically, the overall flood resilience of the study area under the future scenario is 0.6652, a decrease of 0.07% compared with the baseline scenario. The flood resilience of highly urbanized areas under the future scenario is 0.6213, a decrease of 0.50% compared with the baseline scenario. These results imply that, although the overall changes in flood resilience within the study area are slight under the low-forcing scenario in the near future, climate change still negatively affects the capacity of the study area to maintain its functional state, with effects more pronounced in highly urbanized areas.

Figure 5 offers additional evidence supporting the above interpretation. Taking the flood resilience distribution in 2019 as the baseline, changes in flood resilience under SSP1-2.6 in 2070 show that, over half of the study area (57%) is projected to experience a decline in flood resilience by 2070, with affected zones primarily concentrated in the eastern, central, and western parts of the PRD. In highly urbanized areas, flood resilience is expected to decrease across most of the territory. Generally, even under a low-forcing scenario consistent with a sustainable development pathway, climate change continues to negatively affect the flood resilience in most parts of the PRD, with the impact being more evident in highly urbanized areas than in less urbanized ones. The regions showing increased flood resilience are primarily located in Zhaoqing, Jiangmen, and Huizhou. According to Fig. 1 and the calculation principles of the ECPM, the negative impacts of precipitation on flood resilience in these regions in 2070 are reduced compared with 2019, thereby enhancing flood resilience in the future.

Fig. 5 Changes in flood resilience under SSP1-2.6 in 2070 compared with 2019.

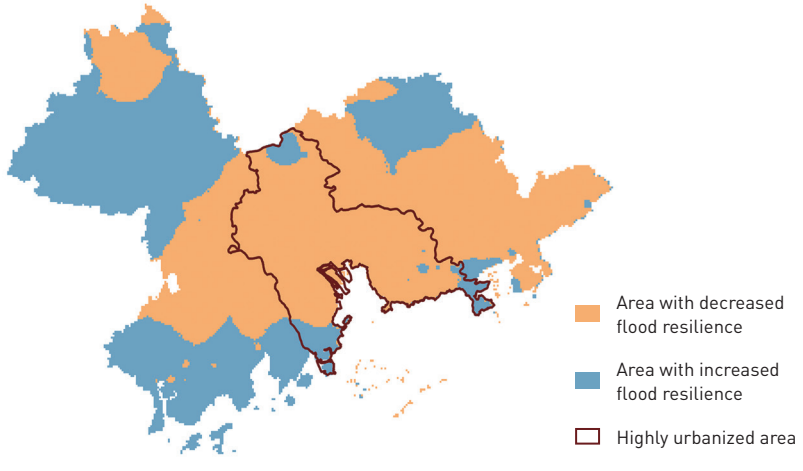

4.2 Multi-level Flood Resilience Enhancement Pathway

Based on the responses of multi-scale flood resilience to climate change, a multi-level flood resilience enhancement pathway was proposed. Analyses at the urban agglomeration scale indicate that highly urbanized areas are more sensitive to climate change in terms of flood resilience and should therefore be given prioritized in resilience enhancement. From a top-down perspective of "urban agglomeration–economic circle–city," highly urbanized areas in the PRD span across three economic circles; at the economic circle level, enhancing flood resilience within highly urbanized areas should first target the SDH economic circle. By further considering the responses of flood resilience to climate change across different cities and economic circles, enhancing Dongguan's flood resilience is crucial for improving that of the PRD under climate change. Accordingly, priority measures should be directed toward Dongguan, thereby constructing a multi-level pathway of "highly urbanized areas–the SDH economic circle–Dongguan" for flood resilience enhancement. For the specific measures to be adopted at each level within the top-down approach to enhancing flood resilience, highly urbanized areas can first establish a regional flood control coordination system and set up a framework for flood resilience enhancement goals and plans. Under the guidance of this framework, the SDH economic circle can further identify key resilience enhancement regions within its member cities and strengthen flood control functions for different land uses. On this basis, Dongguan can develop detailed flood resilience enhancement schemes for the key areas designated by the SDH economic circle, prioritizing investment and infrastructure layout accordingly.

5 Conclusions

First, the ranking of cities by flood resilience, arranged from highest to lowest, is Zhaoqing, Shenzhen, Jiangmen, Huizhou, Zhuhai, Zhongshan, Guangzhou, Foshan, and Dongguan in both the 2019 and the 2070 SSP1-2.6 scenarios. The response of flood resilience to climate change is most pronounced in Zhuhai, but least pronounced in Shenzhen. Climate change impedes the maintenance

of flood resilience in most cities in the PRD, even under a low-emission scenario on a sustainable development path.

Second, the ranking of economic circles by flood resilience, arranged from highest to lowest, is the GFZ, the ZZJ, and the SDH economic circles in both the 2019 and the 2070 SSP1-2.6 scenarios. Climate change exerts the strongest impacts on the flood resilience of the SDH economic circle, followed by the ZZJ economic circle, while its impacts on the GFZ economic circle are the weakest. Climate change undermines the capacity of the two largest economic circles in the PRD to maintain flood resilience, even under a low-emission scenario on a sustainable development path.

Third, the overall flood resilience of the study area under the future scenario is 0.6652, a decrease of 0.07% compared with the baseline scenario. The flood resilience of highly urbanized areas under the future scenario is 0.6213, a decrease of 0.50% compared with the baseline scenario. From the perspective of urban agglomeration, although the overall changes in flood resilience are slight under the low-forcing scenario consistent with a sustainable development pathway, climate change continues to negatively impact the capacity to maintain flood resilience in most parts of the PRD, with the impact being more evident in highly urbanized areas than in less urbanized areas.

Finally, the PRD should establish a top-down approach of "highly urbanized areas–the SDH economic circle–Dongguan" for multi-level flood resilience enhancement. Enhancing the flood resilience of Dongguan is of significant importance for achieving flood resilience enhancement in the PRD under climate change.

Although this study provides insights into multi-scale flood resilience responses to climate change and multi-level flood resilience enhancement pathways, it examines flood resilience in the PRD for only two representative years (i.e., 2019, 2070), without considering the interannual variations over a long time series. As a result, it cannot fully capture the dynamic response patterns of flood resilience at different spatial scales under evolving climate change impacts more precisely. Future research could incorporate long-term time series to refine this study by examining the interannual variability of flood resilience across multiple urban scales. This would support the development of more targeted and effective pathways and measures for flood resilience enhancement at various administrative levels, and further deepen understandings of the response patterns of flood resilience to climate change.

Competing interests | The authors declare that they have no competing interests.

REFERENCES

[1] Xu, Z., & Li, P. (2022). Progress on hydrological response to urbanization: Mechanisms, methods and solutions. *Water Resources Protection*, *38*(1), 7–17.

[2] Chan, F. K. S., Paszkowski, A., Wang, Z., Lu, X., Mitchell, G., Tran, D. D., Warner, J., Li, J., Chen, Y. D., Li, N., Pal, I., Griffiths, J., Chen, J., Chen, W.-Q., & Zhu, Y.-G. (2024). Building resilience in Asian mega-deltas. *Nature Reviews Earth & Environment*, *5*(7), 522–537.

[3] Zhou, T., Zou, L., & Chen, X. (2019). Commentary on the Coupled Model Intercomparison Project Phase 6 (CMIP6). *Climate Change Research*, *15*(5), 445–456.

[4] Zhang, L., Chen, X., & Xin, X. (2019). Short commentary on CMIP6 Scenario Model Intercomparison Project (ScenarioMIP). *Climate Change Research*, *15*(5), 519–525.

[5] Chen, X., Zhang, H., Chen, W., & Huang, G. (2021). Urbanization and climate change impacts on future flood risk in the Pearl River Delta under shared socioeconomic pathways. *Science of the Total Environment*, *762*, 143144.

[6] Hundecha, Y., Sunyer, M. A., Lawrence, D., Madsen, H., Willems, P., Bürger, G., Kriaučiūnienė, J., Loukas, A., Martinkova, M., Osuch, M., Vasiliades, L., von Christierson, B., Vormoor, K., & Yücel, I. (2016). Inter-comparison of statistical downscaling methods for projection of extreme flow indices across Europe. *Journal of Hydrology*, *541*, 1273–1286.

[7] Yang, Y., Chen, L., & Shen, B. (2021). Dynamic-statistical downscaling method for annual precipitation prediction in Yangtze River Basin and its application. *Transactions of Atmospheric Sciences*, *44*(6), 835–848.

[8] Yao, Z., & Huang, G. (2024). Effects of multiple future environmental changes on flooding in coastal area: Case study in Qianshan River Basin, South China. *Journal of Hydrology*, *634*, 131116.

[9] Zheng, J., Chen, X., Kawaike, K., Yamanoi, K., Koshiba, T., & Huang, G. (2024). Response of urban flood resilience to climate change: An exploration with a novel performance-based metric considering the socioeconomic impacts of damage costs. *Journal of Hydrology*, *645*, 132260.

[10] Yao, Z., & Huang, G. (2025). Adaptability comparison of climate downscaling methods and future climate projections in the Pearl River Delta, China. *Natural Hazards*, *121*, 4703–4729.

[11] Chen, J. (2021). *Research on flood disaster risk assessment methods in urbanized areas under different spatial scales* [Master's thesis]. South China University of Technology.

[12] Wang, Y., Meng, F., Liu, H., Zhang, C., & Fu, G. (2019). Assessing catchment scale flood resilience of urban areas using a grid cell based metric. *Water Research*, *163*,114852.

[13] Chen, J., Chen, W., & Huang, G. (2021). Assessing urban pluvial flood resilience based on a novel grid-based quantification method that considers human risk perceptions. *Journal of Hydrology*, *601*, 126601.

[14] Chen, W., Lei, Y., Qi, L., Zheng, J., Huang, G., & Wang, H. (2024). Understanding the evolution trend of urban flood risk and resilience for better flood management. *Ecological Indicators*, *169*, 112829.

[15] Liu, G., Yuan, X., Huang, J., & Wang, H. (2018). Evaluation of urban

resilience to flood based on PSR framework—A case of area in Suzhou–Wuxi–Changzhou. *Resource Development & Market*, *34*(5), 593–598.

[16] Ji, J., Chen, J., & Zhou, Z. (2022). Research on urban flood resilience evaluation and influencing factors in Jiangsu Province. *Journal of Economics of Water Resources*, *40*(4), 48–54.

[17] de Moel, H., Jongman, B., Kreibich, H., Merz, B., Penning-Rowsell, E., & Ward, P. J. (2015). Flood risk assessments at different spatial scales. *Mitigation and Adaptation Strategies for Global Change*, *20*, 865–890.

[18] Wang, K., Zhang, H., Li, G., Zhang, C., Wang, H., Mu, J., & Wang, G. (2023). Advances in urban flood resilience study and its key supporting technologies review. *Water Resources and Hydropower Engineering*, *54*(11), 77–88.

[19] Li, Y. (2017). *The urban disaster resilience assessment and evaluation research* [Master's thesis]. Nanjing University.

[20] Huang, G., Li, D., Zhu, X., & Zhu, J. (2021). Influencing factors and their influencing mechanisms on urban resilience in China. *Sustainable Cities and Society*, *74*, 103210.

[21] World Bank Group. (2015, January 25). *East Asia's changing urban landscape: Measuring a decade of spatial growth*.

[22] Liu, Z., Huang, H., Werners, S. E., & Yan, D. (2016). Construction area expansion in relation to economic-demographic development and land resource in the Pearl River Delta of China. *Journal of Geographical Sciences*, *26*(2), 188–202.

[23] Chen, Y. (2021). *Variation characteristics of rainfall and flood risk in Pearl River Delta during urbanization* [Master's thesis]. South China University of Technology.

[24] Zhang, H., Wu, C., Chen, W., & Huang, G. (2019). Effect of urban expansion on summer rainfall in the Pearl River Delta, South China. *Journal of Hydrology*, *568*, 747–757.

[25] Yao, Z., Huang, G., & Chen, Z. (2023). Effect of land-use changes in different urbanization periods on flooding in Qianshan River Basin, South China. *Journal of Hydrologic Engineering*, *28*(9), 05023015.

[26] Abualkishik, A. Z. (2018). A comparative study on the software architecture of WRF and other numerical weather prediction models. *Journal of Theoretical and Applied Information Technology*, *96*(24), 8244–8254.

[27] Zhang, H., Qiu, J., Huang, B., Yang, Z., & Cai, Y. (2022). Impact of climate change on drainage system of typical urban watershed in Pearl River Delta. *Water Resources Protection*, *38*(6), 56–63, 193.

[28] Zheng, J., & Huang, G. (2023). Towards flood risk reduction: Commonalities and differences between urban flood resilience and risk based on a case study in the Pearl River Delta. *International Journal of Disaster Risk Reduction*, *86*, 103568.

[29] Li, W., Jiang, R., Xie, J., Zhu, J., Zhao, Y., & Yang, S. (2022). Scenario analysis of urban waterlogging disaster based on PSR and Bayesian network. *Water & Wastewater Engineering*, *48*(4), 125–131.

[30] Ji, J., & Chen, J. (2022). Urban flood resilience assessment using RAGA-PP and KL-TOPSIS model based on PSR framework: A case study of Jiangsu Province, China. *Water Science & Technology*, *86*(12), 3264–3280.

[31] Li, N., Liu, W., & Gao, H. (2019). A comprehensive assessment of the economic growth based on extension catastrophe progression method. *Journal of Guangdong University of Technology*, *36*(3), 8–15.

[32] Li, N. (2019). *Extension catastrophe progression method and its application* [Master's thesis]. Dalian Maritime University.

[33] Xu, F., Qu, Y., Bento, V. A., Song, H., Qiu, J., Qi, J., Wan, L., Zhang, R., Miao, L., Zhang, X., & Wang, Q. (2024). Understanding climate change impacts on drought in China over the 21st century: A multi-model assessment from CMIP6. *npj Climate and Atmospheric Science*, *7*, 32.

[34] Panagos, P., Borrelli, P., Matthews F., Liakos, L., Bezak, N., Diodato, N., & Ballabio, C. (2022). Global rainfall erosivity projections for 2050 and 2070. *Journal of Hydrology*, *610*, 127865.

[35] Kain, J. S., & Fritsch, J. M. (1993). Convective Parameterization for Mesoscale Models: The Kain-Fritsch Scheme. In: *The Representation of Cumulus Convection in Numerical Models* (pp. 165–170). American Meteorological Society.

[36] Iacono, M. J., Delamere, J. S., Mlawer, E. J., Shephard, M. W., Clough, S. A., & Collins, W. D. (2008). Radiative forcing by long-lived greenhouse gases: Calculations with the AER radiative transfer models. *Journal of Geophysical Research Atmospheres*, *113*, D13103.

[37] Chen, F., & Dudhia, J. (2001). Coupling and advanced land surface–hydrology model with the Penn State–NCAR MM5 modeling system. Part I: Model implementation and sensitivity. *Monthly Weather Review*, *129*, 569–585.

[38] Hong, S.-Y., Noh, Y., & Dudhia, J. (2006). A new vertical diffusion package with an explicit treatment of entrainment processes. *Monthly Weather Review*, *134*, 2318–2341.

[39] Lin, Y.-L., Farley, R. D., & Orville, H. D. (1983). Bulk parameterization of the snow field in a cloud model. *Journal of Climate and Applied Meteorology*, *22*, 1065–1092.

[40] Hou, T., Zhu, Y., Lü, H., Sudicky, E., Yu, Z., & Ouyang, F. (2015). Parameter sensitivity analysis and optimization of Noah land surface model with field measurements from Huaihe River Basin, China. *Stochastic Environmental Research and Risk Assessment*, *29*, 1383–1401.

[41] Danumah, J. H., Odai, S. N., Saley, B. M., Szarzynski, J., Thiel, M., Kwaku, A., Kouame, F. K., & Akpa, L. Y. (2016). Flood risk assessment and mapping in Abidjan district using multi-criteria analysis (AHP) model and geoinformation techniques, (cote d'ivoire). *Geoenvironmental Disasters*, *3*, 10.

[42] Huang, G., Luo, H., Chen, W., & Pan, J. (2019). Scenario simulation and risk assessment of urban flood in Donghaochong basin, Guangzhou. *Advances in Water Science*, *30*(5), 643–652.

[43] Chen, J., Huang, G., & Chen, W. (2021). Towards better flood risk management: Assessing flood risk and investigating the potential mechanism based on machine learning models. *Journal of Environmental Management*, *293*, 112810.

LAF | https://doi.org/10.15302/J-LAF-2026-0004
第14卷 / 第1期 / 260004 / 2026
收稿日期 | 2025-04-05　录用日期 | 2025-08-29
中图分类号 | TU984　文献标识码 | A

城市洪涝韧性对气候变化的响应及其多层级提升路径

郑嘉璇[1,2,*]，姚芝军[3]，廖向华[4]，黄国如[4,5,6]，陈茜[7]

1 清华大学土木水利学院水利水电工程系，北京 100084
2 清华大学水圈科学与水利工程全国重点实验室，北京 100084
3 广东省建筑科学研究院集团股份有限公司，广州 510500
4 华南理工大学土木与交通学院，广州 510640
5 华南理工大学亚热带建筑与城市科学全国重点实验室，广州 510640
6 广东省水利工程安全与绿色水利工程技术研究中心，广州 510640
7 日本京都大学工学研究科社会基盘工学专攻，京都 612-8235

***通信作者**
地址：北京市海淀区双清路30号清华大学新水利馆
邮编：100084
邮箱：zhengjx@mail.tsinghua.edu.cn

摘要

受气候变化影响，全球范围内洪涝等极端灾害事件频发。为缓解日益增加且不断变化的洪涝灾害风险并推动韧性城市建设，城市洪涝韧性概念在防灾减灾中得到广泛推广。探究多尺度下城市洪涝韧性对气候变化的响应情况有助于决策者构建多层级洪涝韧性提升路径并提出具体措施，为气候变化下的城市洪涝风险管理提供参考。然而，现有研究仍较为缺乏。为此，本文以珠三角地区为研究区域，基于压力－状态－响应模型和可拓突变级数法，评估了2019年及SSP1-2.6未来气候情景下2070年的城市洪涝韧性水平。研究从城市、经济圈、城市群的视角出发，揭示了多尺度城市洪涝韧性对气候变化的响应，并探究了多层级洪涝韧性提升路径。结果表明：研究区域内，珠海的洪涝韧性对气候变化的响应最明显，深圳则最不明显；气候变化对“深莞惠”经济圈的洪涝韧性的影响最强，对“广佛肇”经济圈的影响最弱。在所有尺度下，即便在可持续发展的低强迫排放情景下，气候变化对珠三角地区内各尺度区域维持洪涝韧性均造成了一定的负面影响，在高度城镇化地区尤甚。因此，珠三角地区应形成“高度城镇化地区－深莞惠－东莞市”的自上而下城市洪涝韧性多层级提升路径。同时，提升东莞的洪涝韧性对实现气候变化下珠三角地区的整体洪涝韧性提升具有重要意义。

关键词

城市洪涝韧性；气候变化；多层级；压力－状态－响应模型；珠三角地区

文章亮点

- 从城市、经济圈、城市群尺度分析洪涝韧性对气候变化的响应
- 提出珠三角地区多层级洪涝韧性提升路径
- 气候变化对不同尺度城市地区的洪涝韧性均有负面影响
- 提升珠三角地区的洪涝韧性应重点关注东莞市

基金项目

- 国家自然科学基金（编号：52279015）
- 亚热带建筑与城市科学全国重点实验室自主研究课题（编号：2023ZA01）